J. Anat. (1965), **99**, 4, pp. 761–790
With 15 figures
Printed in Great Britain

Correlation between nuclear morphology and somatotopic organization in ventro-basal complex of the raccoon's thalamus

W. I. WELKER* AND J. I. JOHNSON, JR.†
Laboratory of Neurophysiology,
University of Wisconsin Medical School, Madison, Wisconsin

The aggregation of nerve cell bodies into architecturally distinct populations, and the gathering of axons into discrete laminae or bundles, are fundamental organizational events within the central nervous system. The thalamic nuclear groups of mammals provide examples of such types of cellular and axonal assemblies. In some mammals, such as the raccoon, the ventro-basal nuclear complex (*Vb*) exhibits unusually clear patterns of cellular clustering and axonal lamination. Questions regarding the functional significance of these morphological formations have long been the province of neuroanatomists, but microelectrode recording techniques now permit more direct investigation of the physiological meaning of these specific neural structures. We undertook, therefore, to determine whether the several subnuclei and fibrous laminae in the raccoon's ventro-basal thalamic region exhibit distinct physiological characteristics. Utilizing electrophysiological recording, and ablational, as well as descriptive neuroanatomical methods, our studies have shown that each subnucleus of this somatic sensory complex not only receives projections from mechanoreceptors in distinct body parts, but also projects its primary axons to distinct gyral crowns within somatic sensory (*SmI*) neocortex.

MATERIALS AND METHODS

Twelve raccoons (*Procyon lotor*) of both sexes were used in electrophysiological recording, thirteen in retrograde degeneration, and six in Wallerian degeneration (Marchi method) experiments. All these animals were within the adult or young adult range of body and brain size.

Electrophysiological recording procedures

Animal preparation. All animals were anaesthetized with pentobarbital sodium (initial dose: 40 mg./kg. of body weight) administered intraperitoneally, supplemented when necessary to eliminate nociceptive reflexes. The body hair was clipped to within 1–2 mm. of the skin surface. The trachea was then cannulated and the head mounted in standard manner in the head holder of a stereotaxic instrument. Scalp and bone were removed and the dura was reflected over a neocortical region sufficiently large to allow vertical access to the underlying thalamic region. In

* Supported by the Sister Kenny Foundation and USPHS (NIH Grant: 5-K3-NB-4892.
† USPHS Special Research Fellow (NIH Grant: MSP-11555).

some cases, the overlying pia-arachnoid and neocortex were aspirated to facilitate smooth penetration of the electrode.

Electrodes. Systematic exploration of the somatic sensory thalamus was carried out in stereotaxic co-ordinates using either macroelectrode stainless steel beading needles (no. 11; Boyle Needle Co., Chicago, Illinois; shaft diameter = 450μ; tip diameter = 30μ) or tungsten microelectrodes prepared by the method described by Hubel (1957). The microelectrodes used had a shaft diameter of about 40–50μ, variably tapered shank shapes, and tip diameters of 2–6μ. The electrodes were insulated to within about 20–30μ of the tip with either Insl-X or Epoxylite varnish.

Recording equipment. The exploring electrode recorded voltages with respect to a reference electrode attached to an exposed portion of the animal's scalp. These two electrodes were attached to the two grids of an Argonaut Differential Preamplifier. The recorded electrical activity was passed through 10 cyc./sec. low, and 10 kcyc. high, cut-off filters. The output from this amplifier was led into the amplifier of a Tektronix 502 oscilloscope. The output from this latter amplifier was displayed visually upon the oscilloscope screen and, with additional amplification, audibly through an 8 in. speaker.

Mapping procedure. A mapping procedure was used throughout and consisted of the following steps: (*a*) The electrode was introduced through the overlying cortex and white matter and advanced into the thalamus in a series of regularly spaced punctures oriented in the frontal plane. (*b*) During the slow passage of the electrode through the thalamus, the animal's body surface was rapidly and thoroughly stroked and manipulated in order to ascertain whether the thalamic units that were encountered could be activated by mechanical stimulation of receptors in skin, muscles, deep tissues, or joints. (*c*) When a 'drivable' thalamic neural unit or a group of such units was encountered, the electrode advance was stopped and the peripheral receptive field or locus which maximally activated the units was carefully delineated. In identifying a peripheral receptive field, only that area was delineated which, with minimal mechanical stimulation, reliably activated thalamic units. (*d*) The peripheral receptive fields so defined at each recording locus were outlined on photographs or figurines of the appropriate body part. Such a figurine was prepared for each responsive 0·5 mm. step in depth along each electrode track. Additional figurines were charted at shorter intervals whenever the focus of a peripheral activating region changed markedly from that which was identified at the usual regular 0·5 mm. location just above it. (*e*) Dorsal and ventral boundaries of the somatic sensory thalamus were established by identifying 'nil' or unresponding loci above and below the responding region. (*f*) Successive electrode punctures were made in regular steps (1 or 0·5 mm. apart) mediolaterally and antero-posteriorly until the entire thalamic region that was responsive to mechanical stimulation of the body had been surrounded by 'nil' punctures in which no peripherally drivable units were encountered, or in which the response characteristics of such units were sufficiently different to suggest that they were within another thalamic region. (*g*) Each responding electrode locus was always identified in the protocol by three numbers, which referred to the respective distances of that locus from the three standard planes of the stereotaxic instrument. This procedure made it possible to reconstruct the thalamic pattern of

representation of mechanoreceptors of the body in coronal, horizontal, or sagittal planes. Although most experiments were carried out in the right side of the thalamus, all data are illustrated as being on the left in the figures.

These collective procedures constituted our *microelectrode method of electrophysiological mapping*. By these means the complete topographic projection of one cellular mosaic (e.g. body receptors) upon another (e.g. thalamic ventro-basal complex) can be precisely determined.

Response criteria. The primary criterion of a responding thalamic locus in the microelectrode experiments was the visible isolation on the oscilloscope screen of unit spike discharges which could be activated by mechanical stimulation of the body.

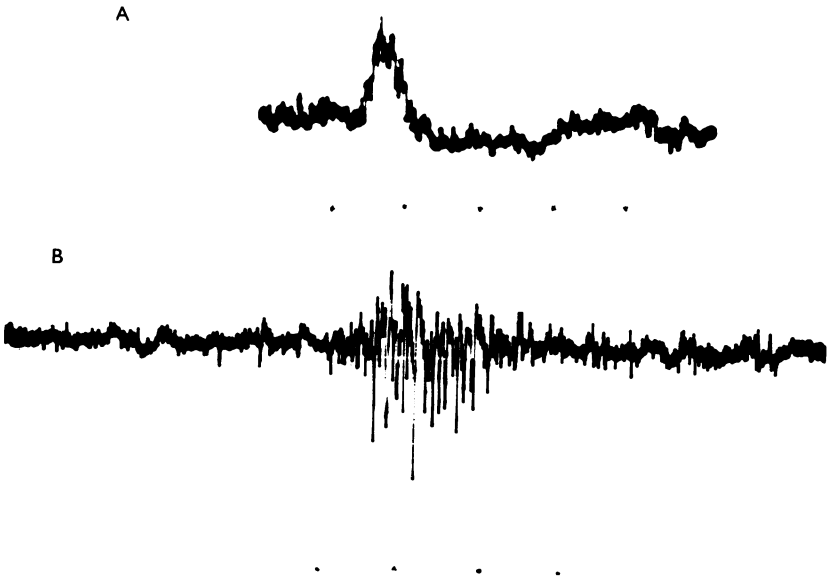

Fig. 1. A. Slow-wave potential evoked in *Vb* thalamus by mechanical stimulation of contra-lateral ankle in raccoon no. 59–264. Time scale = 60 cyc./sec. Recorded by no. 11 stainless steel beading needle. B. Neural unit spike discharge cluster used as response criterion in *Vb* thalamus. Evoked by mechanical stimulation of hairs over lateral aspect of ankle in raccoon no. 63–91. Slow wave filtered out (320 cyc./sec. filter). Time scale = 100 cyc./sec. Recorded by tungsten microelectrode. Positive electrical sign is up in both records.

Those electrodes which were used for mapping would record activity of occasional isolated single units, and of unit clusters, as well as 'neural hash' noises which signal the approach of the electrode tip toward relatively more distantly active units (e.g. those up to 500 μ away). Such audible noise patterns served as valuable signs of the approach of the electrode tip toward the dorsal border of the somatic sensory thalamus, as well as toward a cluster of cells activated from a different peripheral source than that which might have just been encountered (Bishop, Kozak, Levick & Vakkur, 1962; Mountcastle & Henneman, 1952).

Because of the size of the recording electrode tip, it is likely that presynaptic as well as postsynaptic neural electrical activity contributed to these unit cluster

records (see Welker, Johnson & Pubols, 1964). Some of the spikes in these clusters were initially positive, and others initially negative, in electrical sign (Fig. 1B). The largest stable spike responses were initially negative in electrical sign, but this fact in itself is no sure sign that the electrode was recording extracellularly from the soma of a neuron rather than from other elements within such a complex neural matrix (see Bishop, Burke & Davis, 1962; Fatt, 1957; Freygang, 1958; Rose & Mountcastle, 1954; Svaetichin, 1958; Tasaki, Polley & Orrego, 1954).

In the entire series of recording experiments, 747 responding loci were studied along 163 active punctures. Sixty-one 'nil' punctures served to delimit the anterior, posterior, medial, and lateral boundaries of the responding thalamic region.

Anatomical procedures

Histological techniques. At the completion of a recording experiment the brain was perfused with formalin, removed from the skull, and cut coronally at either 40 μ (frozen technique), or at 20–25 μ (paraffin or celloidin embedding technique), and mounted on slides. All sections from the frozen material were stained with cresyl violet. Alternate serial sections from the paraffin material were stained with thionin (for cell bodies) and haematoxylin (for myelin sheaths). The brains of all ablated animals were embedded in celloidin, cut at 25–30 μ, and alternate sections were stained for cell bodies and myelin sheaths. The brain of the digit-3-sparing animal (no. 61–424) was sectioned in the horizontal plane, all others were cut coronally.

Identification of responding locus. The intracerebral electrode punctures or tracks were traced and identified in every case by microscopic examination of serial sections. Identification of the anatomical location of the recording electrode tip along each track was accomplished by one of three methods: (*a*) the fitting, by interpolation (cf. Rose & Mountcastle, 1952), of the recorded data from the protocols to particular locations along the histologically identified electrode track; (*b*) the Prussian Blue method of electrolytic deposition of iron at the location of a recording steel electrode tip (Green, 1958); or (*c*) the production of microlesions at a particular location of the tip of a tungsten microelectrode. Since the interpolation method leaves much to be desired as regards accuracy (Robinson, 1962), the two marking methods were used in some of the recording experiments in order to increase the precision of the histological identification of the physiologically defined boundaries (Akert & Welker, 1961).

Degeneration experiments. Aseptic surgical technique was used in the chronic selective partial ablation of somatic sensory neocortex (*SmI*; Woolsey, 1958) in thirteen raccoons. These ablations were unilateral for each cortical subarea removed, and were performed by the subpial aspiration method. The extent of adequacy of the neocortical lesions was reconstructed by means of microscopic examination of serial sections of the operated brains. The thalamic regions exhibiting retrograde degenerative changes (gliosis; chromatolysis, shrinkage, deformation, and loss, of nerve cells) were similarly reconstructed, and enlarged projected images of these regions of thalamic degeneration were drawn in outline in order to indicate the three-dimensional topographical organization of these various cortically dependent somatic sensory subdivisions within the thalamic

ventro-basal complex. The somatotopic organization of the several degenerated regions defined by this method was then compared with that which was determined by the electrophysiological recording techniques described above.

Wallerian degeneration was studied in six raccoons using the Marchi method (Swank & Davenport, 1935). In these animals, the cuneate, gracile, or spinal trigeminal (Vth) nucleus was ablated unilaterally, or else the midbrain was hemisectioned intercollicularly, 11–16 days before the brains were perfused. The course of the fibres exhibiting degenerating myelin sheaths in these cases was followed microscopically on serial sections through the midbrain and into the diencephalon.

RESULTS

Electrophysiological observations

Since the electrophysiological studies of the ventro-basal thalamic nuclear complex constituted a crucial phase in the anatomical localization of somatic sensory projections within this region, these experiments will be considered first.

Characteristics of evoked activity. When the recording electrode tip entered the thalamic somatic sensory region, the 'neural hash' sounds increased markedly in amplitude and density (i.e. number of unit spikes per unit of time) over those which were recorded in white matter or from other thalamic regions (cf. Mountcastle & Henneman, 1949). Although these sounds appeared to be 'spontaneous', we believe that they may be activated by mechanoreceptors in joints, skin, and deeper tissues which are inevitably stimulated because of respiratory movements, circulatory pulsations, and the particular postures and patterns of contact of the body with the headholder and the table surface. Macroelectrodes were used in the first two thalamic mapping experiments (nos. 58–407 and 59–264). Fig. 1A illustrates the type of evoked slow wave used as response criterion in these experiments. In all the subsequent microelectrode recording experiments, the major criterion of a responding locus was the unit cluster (Fig. 1B). We consider it important to note that the electrodes used seemed to discriminate effectively between fibres of passage and aggregations of cell bodies and neuropil. Thus, only low amplitude signals were recorded within efferent and afferent fibre tracts lateral and caudal to *Vb*, or in fibre laminae or bundles within *Vb*. Presumably, these differences are associated with the higher electrical resistance of myelinated fibre tracts (Robinson, 1962).

Pattern of organization of somatic sensory thalamus. The general three-dimensional organization of the thalamic somatic sensory representation can be determined from inspection of Fig. 2. The thalamic somatic sensory 'procyonculus' may be visualized as standing somewhat erect upon the base of the thalamus; the head, face, and tongue located medially and the tail and hindlimb situated laterally. The representation of the trunk is located at the dorsocaudo-lateral aspect of this region, and those of the apices of the limbs are directed ventrally. This general pattern is similar to that found in the ventro-basal complex of other mammals (see Discussion). The representations of forepaw (hand) digits were found to be arranged in regular order with that of the first digit situated nearest the head, that of the fifth digit just medial to the hindfoot representation. and the other digits

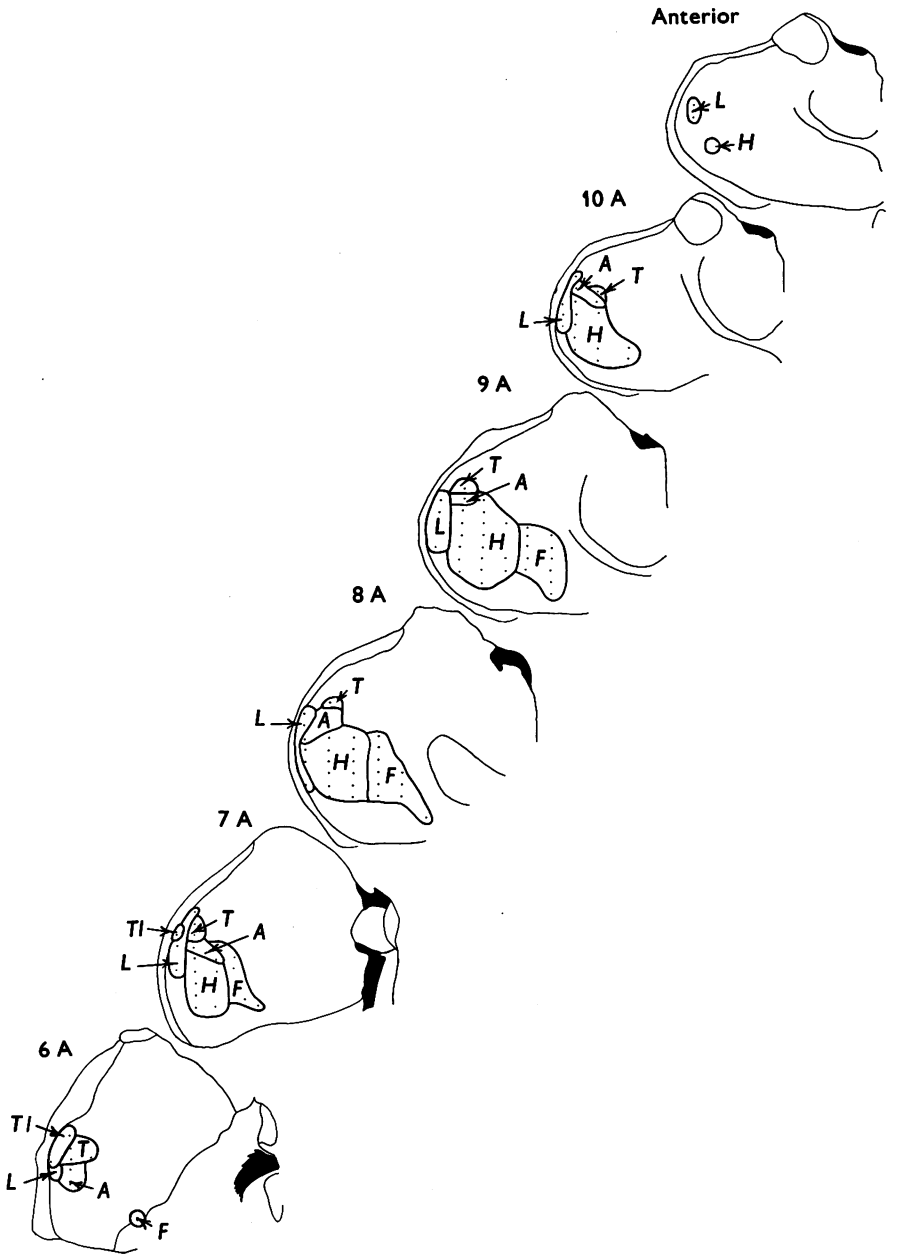

Fig. 2. Diagrammatic reconstruction of right somatic sensory region of thalamus (reversed to appear as left), showing location of representations of several body subdivisions. Animal no. 61–148. Drawings are of six coronal sections 1 mm. apart, which contained electrode tracks. Dots indicate positions of responding loci which were 0·5 mm. apart in dorso-ventral direction and 1 mm. apart medio-laterally. 6A, 7A, etc, refer to stereotaxic co-ordinates. *A*, Arm; *F*, face; *H*, hand; *L*, leg and foot; *T*, trunk; *Tl*, tail.

represented consecutively between them. The thalamic region that was responsive to stimulation of the palm is located dorsocaudally within *Vb* near the representations for the proximal portions of all the forepaw digits. Partial maps from all the other experiments confirmed this general three-dimensional picture in every respect.

Except for the ipsilateral face, mouth, and tongue representations which were located most medially, the responsive units at each thalamic recording site were activated solely by contralateral body stimulation under the conditions of these experiments. Tabulation of the number of responding loci (N-130), from the one experiment depicted in Fig. 2, revealed that the total volume of thalamic neural

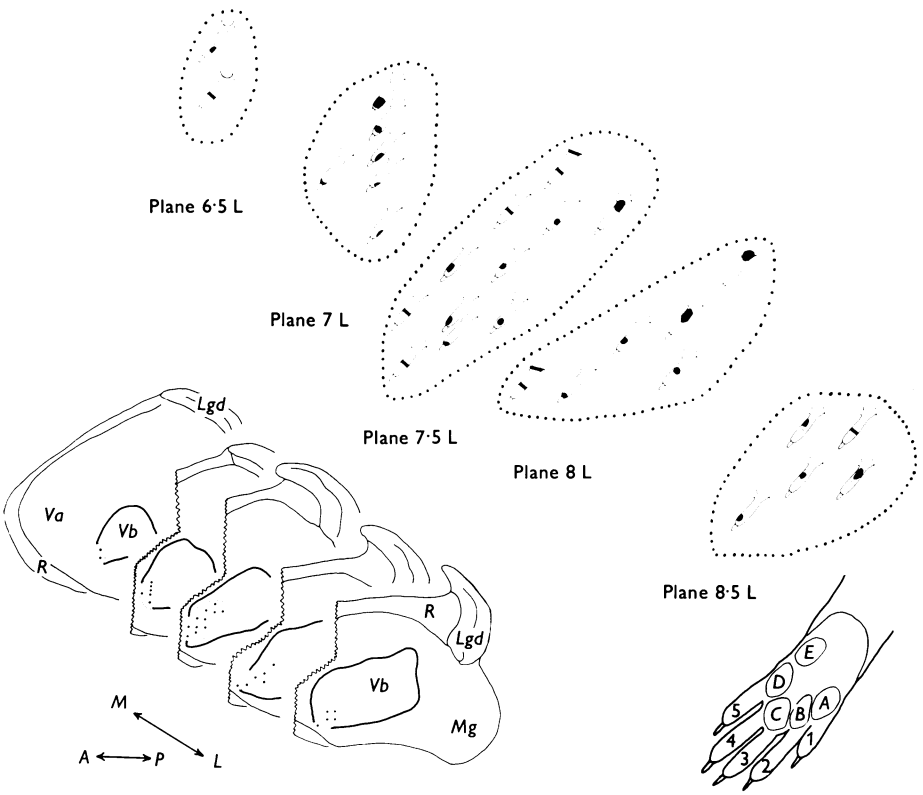

Fig. 3. Sagittal reconstruction of thalamic somatic sensory representation of ventral surface of forepaw digit 3 (experiment no. 61–221). The third-digit figurines placed on the five sagittal planes within *Vb* indicate *AP*, *ML*, and *DV* organization of the digit 3 projections. The inset drawing at lower right is of the ventral surface of raccoon forepaw. Digit figurines are mounted similarly to that of hand figurine so that the ulnar side of the digit is situated more dorsally, and the radial side more ventrally. The radial-ulnar progression of the representation goes medio-laterally. The location of figurine arrays within *Vb* is indicated by diagrams of sagittal sections of thalamus at lower left. *Lgd*, Dorsal lateral geniculate nucleus; *Mg*, medial geniculate nucleus; *Va*, nucleus ventralis anterior; *R*, reticular nuclear complex; *A*, anterior; *L*, lateral; *M*, medial; *P*, posterior. Black patches with rounded contours indicate the locus and relative size of the peripheral region which, when stimulated mechanically, activated units at the particular thalamic locus occupied by the figurine. Solid black bars on a figurine indicate that unit clusters at that locus were evoked primarily by joint movement.

tissue activated by light mechanical stimulation of the body in this animal was about 65 mm.^{3}. About 44% of the recording loci (N-57) within this region was activated by forepaw stimulation.

Because of the relatively wide (1 mm.) spacing of electrode punctures in the experiment just described, certain finer details of the pattern of representation were not readily apparent. A more detailed mapping study of the thalamic region responsive to stimulation of the third digit of the forepaw was carried out, therefore, using a more closely spaced pattern of electrode punctures and recording locations. The data from this experiment were plotted on figurines oriented in the sagittal plane in order to show certain details of the pattern of organization for a single digit (Fig. 3). This figure indicates the relative size of peripheral receptive fields which activated unit clusters within the somatic sensory forepaw region of the thalamus. It also shows that within this region, the representation of the third forepaw digit points antero-ventrally with its radial side lying medially and its ulnar side situated more laterally.

Unit clusters activated by stimulation of the claws for the forepaw digits were always located most ventrally in the thalamus (see Fig. 13), and those responsive to stimulation of joints and deep tissues of the palm and proximal digits were located more dorsally. In this experiment, no thalamic foci were found which responded to stimulation of the dorsal portions of the forepaw digits, but data from other experiments indicated that these responses were obtained more caudally and ventrally within the somatic sensory thalamic region than were those activated by stimulation of the glabrous ventral forepaw surfaces. Since the spikes within a unit response cluster presumably represent activity of several adjacent thalamic cells, we were not able to determine whether thalamic cells activated by peripherally adjacent joint and cutaneous receptors were intermingled or whether they might be grouped into small modality-pure clusters. Despite the fact that several pre- and postsynaptic elements probably contributed to the unit clusters which constituted the response criterion (see Welker *et al.* 1964), the results of these experiments demonstrate a relatively highly detailed somatotopic pattern of organization within the raccoon's *Vb* thalamus. This is especially true of the representation for the glabrous forepaw surfaces.

In all the microelectrode mapping studies of the raccoon's ventro-basal thalamus, no overlap was found in the thalamic projections of certain of those body parts that are actually *separated* from one another at the periphery, such as head and forepaw, forepaw digits 1 and 2, forepaw and hindpaw, or hindpaw and tail. Thus, under the conditions of our experiments, cells activated by head stimulation were never also activated by forepaw stimulation. Such mutually exclusive relationships of representation for several parts of the body which are peripherally distinct have also been shown to exist at the raccoon's somatic sensory neocortex (Welker & Seidenstein, 1959). Conversely, overlapping thalamic projections were found from adjacent body regions which are peripherally contiguous. For example, in its traverse through the somatic sensory thalamus, an electrode which first encountered cells activated by pelvic stimulation at the dorsal aspect of the responsive region might, with progressively deeper penetration, record successively from cells activated by upper leg, lower leg, and foot. Many electrode punctures thus

demonstrated a *continuous shift* of the thalamic representation of peripherally contiguous body parts for at least a portion of the total traverse of the electrode tip (Fig. 12). In contrast to this, however, in many punctures for at least a portion of the track distance, the peripheral loci which activated unit clusters at successive electrode locations within a particular track jumped, in disjunctive fashion, from one distinct body part to another. Thus, units activated by stimulation of digit 3 might be followed, upon further penetration, by other units which were activated by stimulation of digit 4, or, units activated by stimulation of digit 5 of the forepaw might be followed by others deeper in the puncture which were activated by stimulating digit 1 of the hindpaw. Often, when such a *disjunctive shift* occurred, the peripheral loci which activated units at the two adjacent thalamic loci were adjacent to one another on the two peripherally separated parts (Fig. 11). These differences between disjunctive and continuous shifts have been emphasized in some detail here because they are relevant to, and are easily explained by, the anatomical results that are reported below.

Boundaries of somatic sensory thalamus. The thalamic somatic sensory region studied in these experiments was activated primarily by gentle mechanical stimulation of the body (hair movement, skin deformation and joint movement). 'Nil' points and punctures were established on all sides of this region and its boundaries were assumed to be midway between the reactive and the unresponsive loci. Outside the dorsal, ventral, medial, and lateral boundaries, we found, as did Mountcastle & Henneman (1949) in the cat, that 'spontaneous' unit activity was of relatively low spike density and amplitude. Neural units in such regions were also unresponsive to gentle mechanical peripheral stimulation.

Unit cluster responses were occasionally evoked from punctures passing anterior (into the ventro-lateral nuclear complex, *Vl*), as well as posterior (into the posterior nuclear group, *Po*), to the ventro-basal nuclear complex (*Vb*). In contrast to responses evoked in *Vb*, those recorded in the ventro-lateral nuclear region were (*a*) of small amplitude, (*b*) marked by the absence of sharp crackling background sounds, (*c*) produced by stimulation of relatively large and poorly localized peripheral receptive fields, and (*d*) not usually activated by *light mechanical* stimulation. Responding units within the posterior nuclear region were rejected for similar reasons, as well as for the reason that such units could also be activated by vibratory or auditory stimuli or by stimulation of ipsilateral body parts.

Anatomical observations

The anatomical location of the thalamic somatic sensory region was determined by: (*a*) reconstruction of tracks of the recording electrode, (*b*) placement of small marks at electrophysiologically determined boundary zones by means of Prussian Blue and microcoagulation techniques, and (*c*) identification of regions of retrograde degeneration in the thalamus following ablations of *SmI* somatic sensory neocortex. The results obtained by all of these methods corroborate the concept proposed by Rose & Mountcastle (1952, 1959) in showing that the thalamic somatic sensory region which is activated by light mechanical stimulation of the body, projects to *SmI* neocortex and is coextensive with the ventro-basal complex as defined by those authors (1952).

Normal anatomical characteristics of ventro-basal complex. The ventro-basal complex (*Vb*) in raccoons lies in the ventro-lateral portion of the dorsal thalamus approximately midway between its anterior and posterior poles. In coronal (Fig. 4) and horizontal (Fig. 5) sections, *Vb* can be seen to bulge further laterally than do the adjacent ventro-lateral, lateral, and posterior nuclear regions. Fig. 6 shows

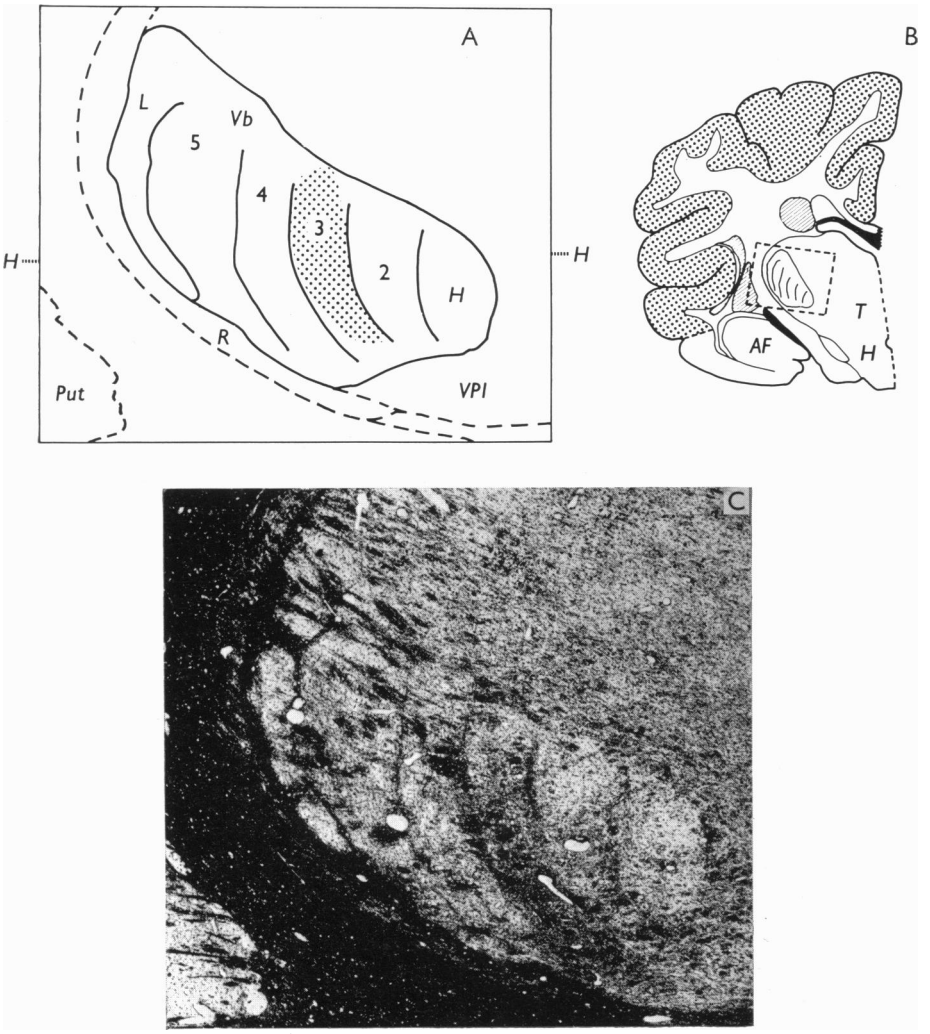

Fig. 4. A, B. Key diagrams showing thalamic location of the transverse section *C*, lobulation of *Vb*, and locus of retrograde degeneration (dotted region) following aspiration of neocortical *SmI* representation of third forepaw digit (see Fig. 8). *Put*, Putamen; *VPI*, ventral posterior-inferior nucleus; *R*, thalamic reticular complex; *L*, *5*, *4*, *3*, *2*, *H*, leg, forepaw digits 5, 4, 3, 2, and head subdivisions of *Vb*, as determined by recording and retrograde degeneration experiments; *AF*, Ammon's formation; *H*, hypothalamus; *T*, thalamus; *H–H*, approximate level of horizontal section of Fig. 5; *C*, coronal section no. 750 of left *Vb* complex of raccoon no. 58–128. Haematoxylin stain (Weil). ×23. (Reproduced with permission of Editor, *American Zoologist*.)

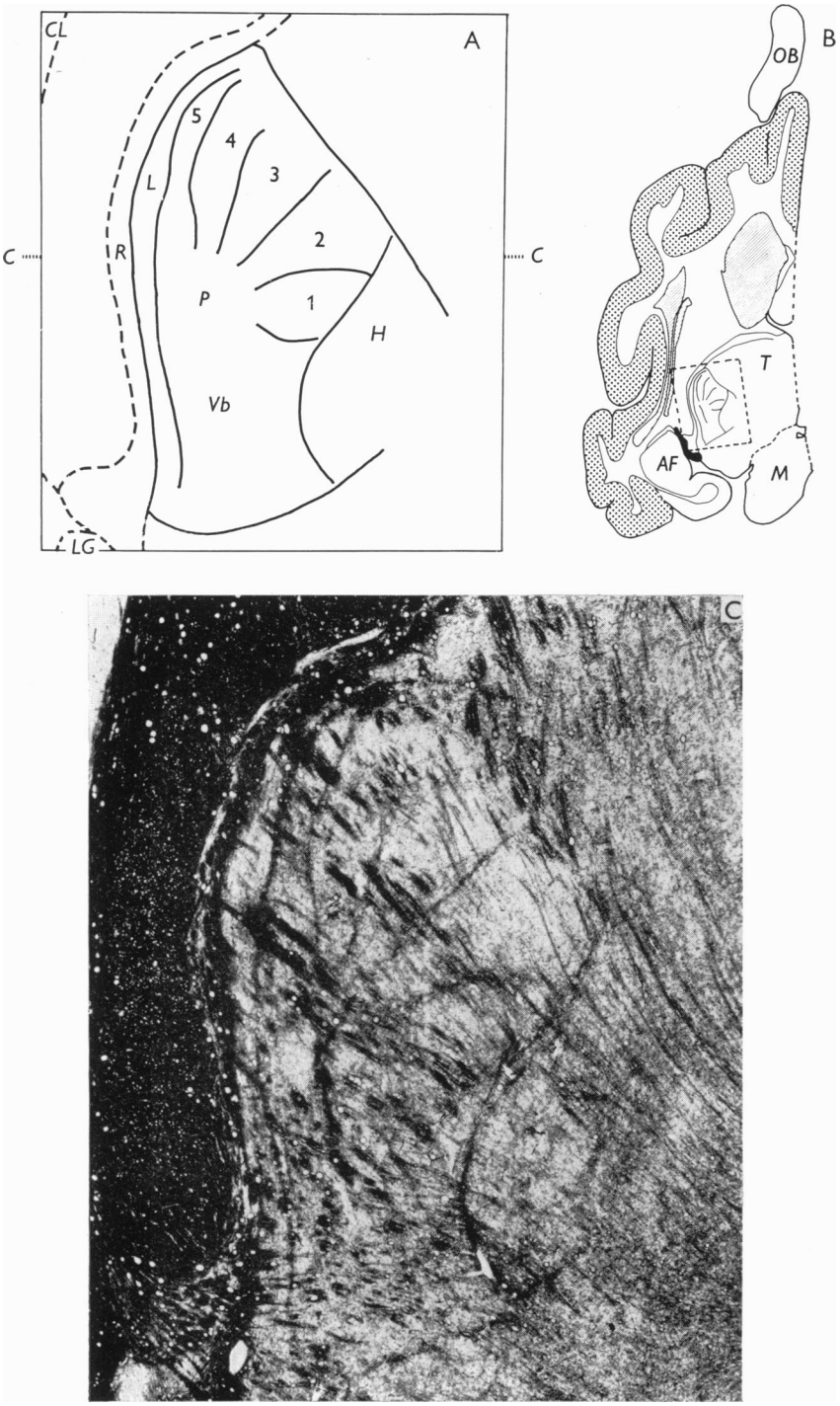

Fig. 5. A, B. Key diagrams showing location of the horizontal section *C*, and lobulation of *Vb*. *CL*, claustrum; *LG*, lateral geniculate nucleus; *M*, midbrain. Other symbols as in Fig. 4. *C–C*, approximate level of coronal section of Fig. 4; C, horizontal section no. 485 of right *Vb* complex (reversed to appear on left) of raccoon no. 57–115. Haematoxylin stain (Weil). ×21.2. (Reproduced with permission of Editor, *American Zoologist*.)

a three-dimensional reconstruction of the *Vb* nuclear region within the left dorsal thalamus. The *Vb* complex is bounded laterally by the thalamic reticular complex, and is largest in both antero-posterior (*AP*) and dorso-ventral (*DV*) directions most laterally. Medially, this complex lies beneath the lateral wings of the centrum medianum. The normal cytoarchitectural characteristics of *Vb* are rather distinct from those in the other thalamic nuclear groups which surround it, except along

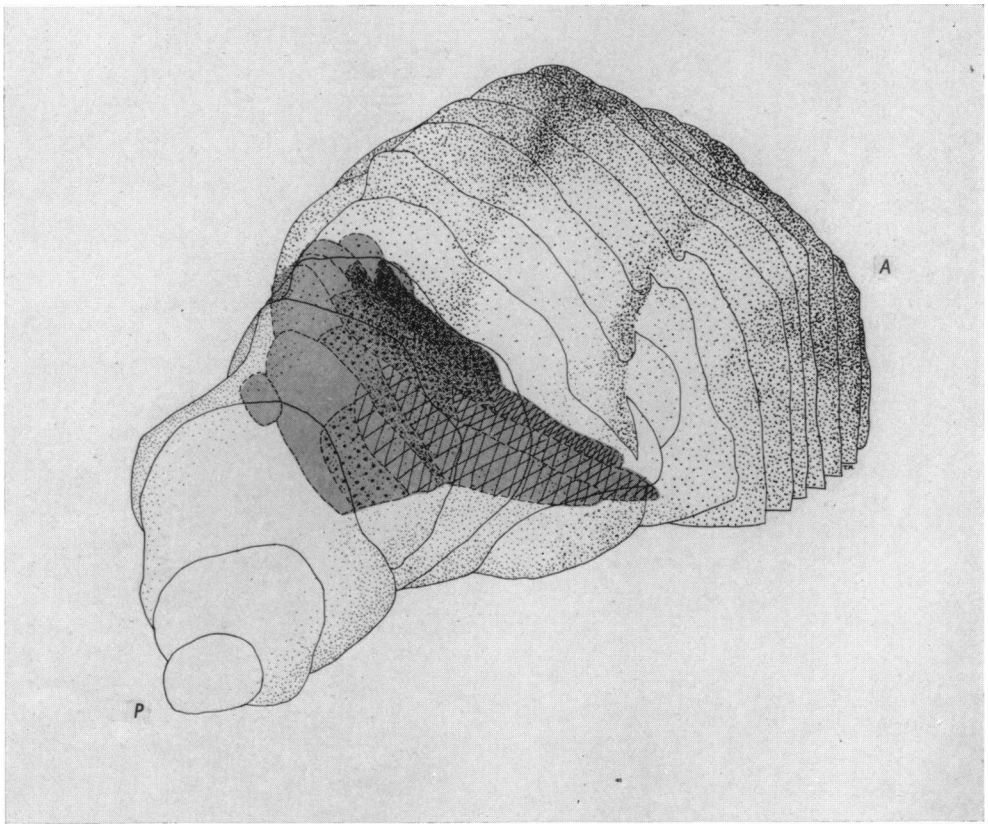

Fig. 6. Reconstruction of left dorsal thalamus of raccoon no. 57–88. The location of the ventro-basal nuclear complex within the thalamus is indicated by the seven gray sections. Shading symbols within *Vb*: *clear region* (located most laterally), tail, hindlimb, trunk, and upper arm regions; *dotted region*, forepaw region; *cross hatched* (located most medially), head region. Geniculate bodies appear as eminences at postero-lateral aspect of thalamus: *A*, anterior; *P*, posterior. (Reproduced with permission of Editor, *American Zoologist*.)

certain portions of: (*a*) the ventro-medial aspects of the head (pars arcuata) region, (*b*) the dorso-medial aspect of the body (pars externa) region, (*c*) the posterolateroventral aspect of pars externa (adjacent to *VPi*), and (*d*) the posterior regions between *Vb* and the medial geniculate region. The boundaries in these indistinct zones were defined primarily by data from the retrograde degeneration experiments.

The anterior pole of *Vb* is distinguished from the ventro-lateral (*Vl*) and the

ventral anterior (*Va*) nuclei by: (*a*) its greater cell density, (*b*) its greater disruption by relatively large fibre fascicles oriented in the medio-lateral direction, (*c*) the irregular clustering of its component cell bodies, (*d*) the greater apparent variability in size of its component cells, and (*e*) the generally darker staining (thionin) of the Nissl substance of its cells, and in some brains, of its neuropil. Similar criteria characterize the differentiation of the dorsal and ventral boundaries. The characteristics mentioned above are exhibited primarily by the external (*ext*), and the lateral portion of the arcuate (*arc*), subdivisions of *Vb*. However, the most medial aspect of the arcuate portion of *Vb* appears to contain a greater proportion of less darkly stained smaller sized cells than are found in the lateral arcuate or external portions of *Vb*. These more medial cells also appear to be more evenly distributed than are those elsewhere.

The patterns of myelinated fibre bundles within *Vb* are of interest because they suggest different modes of organization of its afferent and efferent fibres. One system of relatively heavily myelinated fibres is oriented in a medio-lateral direction. These fibres penetrate the thalamic reticular nuclear complex and enter the internal capsule. They gather into bundles which are larger at the lateral aspect of *Vb* than they are medially (Figs. 4 and 5). They presumably contain the thalamic efferents which reach *SmI* neocortex, as well as some cortico-thalamic fibres. The fact that these fibre bundles are larger laterally than they are medially suggests that fibres from successively more lateral regions become grouped with fibres of passage deriving from, or entering, the more medial thalamic regions. This progressive increase in fibre density in the successively more lateral regions of *Vb* is associated with a gradual medio-lateral decrease in cell density (Welker *et al.* 1964). Except for the aggregation of these fibre bundles, all of which are oriented generally in a medio-lateral direction, they do not exhibit a laminar arrangement. Rather, reconstructions of serial sections in this region indicate that they emerge from the lateral surface of the thalamus in a heterogeneous, irregular, scattered pattern. The manner in which these fibre bundles leave *Vb* suggests that axons from widely separated representations within *Vb* come to lie adjacent to one another within the internal capsule. In contrast with these fibre bundles, the fibres which ascend from the medulla via the medial lemniscus and terminate in *Vb* exhibit an entirely different organization. These afferent fibre bundles or fascicles apparently become grouped into curviplanar sheets or laminae near their loci of termination within the thalamus. They appear to be less heavily myelinated than the thalamocortical fibres. These fibre laminae are oriented roughly parallel to the sagittal plane and transect the thalamocortical and corticothalamic fibre bundles described above at approximately right angles (Figs. 4 and 5). Such a fibre lamina separates the arcuate from the external portion of *Vb* in cats (Mountcastle & Henneman, 1949), and monkeys (Mountcastle & Henneman, 1952). Raccoons also exhibit such an arcuate lamina (Figs. 4, 5, 8 and 9), but have, in addition, several other such laminae which give *Vb* a lobulated appearance in either coronal (Figs. 4, 11 and 13) or horizontal (Figs. 5 and 9) sections. These lobules or subnuclei consist of clusters of cell bodies separated from one another by the fibre laminae. These lobular and laminar characteristics are more prominent in the *Vb* nuclear complex than in the thalamic nuclear regions which surround it on all sides.

The anterograde degeneration (Marchi) experiments show that fibres from the medial lemniscus reach the ventropostero-lateral aspect of the dorsal thalamus, and terminate within the ventro-basal nuclear complex. The lemniscal fibres plunge into *Vb* in a scattered pattern from posterior, lateral, ventral, and medial aspect of this nuclear complex in a manner similar to that described for *Macaca mulatta* by Clark (1936). Since the lemniscal fibres appear to approach *Vb* in a rather dispersed manner from several directions, we advance the hypothesis that the vertically oriented fibre laminae consist of the preterminal myelinated fibres which are becoming sorted out, on a somatotopic basis, just before they make contact with the somatotopically organized thalamic cell groups. If fibres from the medial lemniscus passed into *Vb* solely from its caudal aspect, and if the laminae consisted

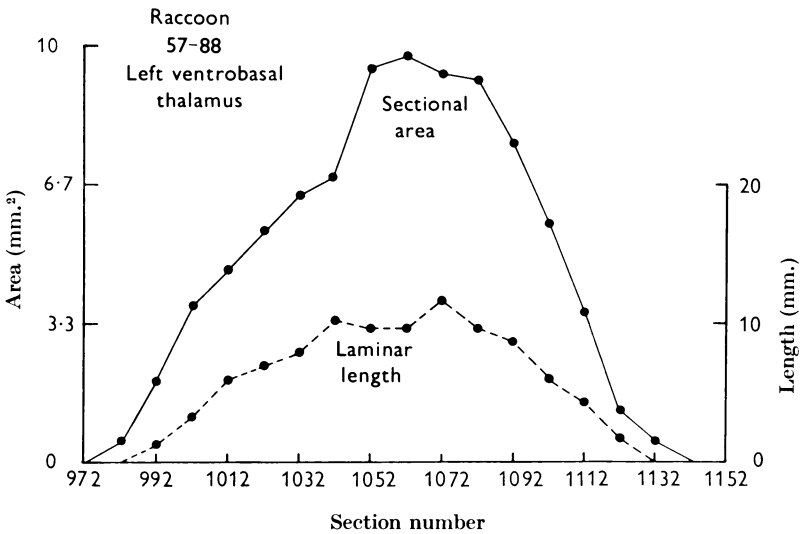

Fig. 7. Graph showing relationships between the cross sectional area (in mm.²) of *Vb* at ten coronal planes, and the total linear length (in mm.) of fibrous laminae within *Vb* at corresponding levels. Anterior is to the left.

primarily of such fibres of passage, then the laminae would be expected to be more prominent or numerous in the caudal portions of this nuclear complex. Fig. 7 shows, however, that the total linear length of the laminae at any given plane is positively correlated with the cross sectional area of *Vb* at that plane of section. Thus, laminar organization is more pronounced in the larger *Vb* regions which presumably receive correspondingly greater numbers of lemniscal afferents that are unshuffling and converging upon their appropriate thalamic subnuclei. The microdetails of these terminations are not yet known although silver-stained sections (Bodian) through this region show that the fibrous laminae within *Vb* contain some horizontally (*AP*), and dorsally, as well as obliquely oriented fibres that appear to enter the subnuclei on either side of a particular lamina.

Thalamocortical anatomical relationships. The fact that several subdivisions of *SmI* neocortex are reliably indicated by the location of neocortical sulci (Fig. 10) encouraged us to study the topographic organization of those thalamic cells which

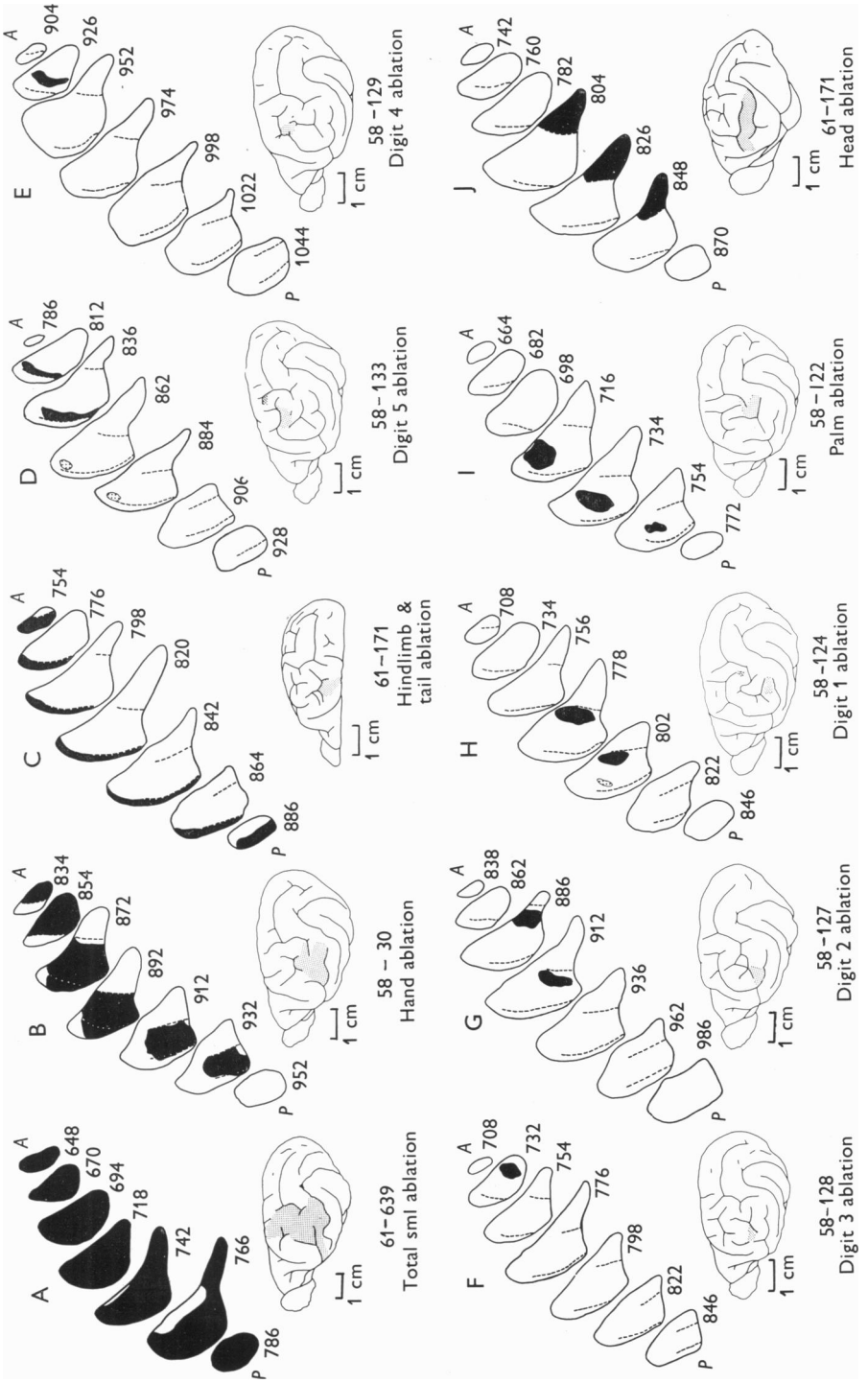

Fig. 8. Reconstruction of loci of thalamic retrograde degenerative changes in *Vb* following aspiration of several neocortical *SMI* subdivisions in nine animals. Brain diagrams indicate locations of cortical lesions (dotted regions). Schematic drawings of coronal sections through seven levels of *Vb* in each case show locations of degenerative changes (black regions) in relation to the arcuate (more medial) fibrous lamina and the more lateral lamina between hindlimb and forepaw representations. Both lamina indicated by dashed lines. In two cases (D, H), small unintended neocortical lesions are indicated in thalamus as well as at cortex by dotted patches. Comparison of all these cases indicates the three-dimensional relationships of the degenerated thalamic subdivisions. For uniformity, all drawings are shown as on left side although some lesions and degenerations were in right hemisphere. C and J show data from the same animal. *Vb* sections displayed in similar orientation as those represented in Fig. 6. *A*, Anterior; *P*, posterior. Section numbers are indicated.

send their axons to these spatially distinct neocortical subdivisions of *SmI*. This was done by the retrograde degeneration method. The thalamic regions which show degenerative changes after unilateral ablation of various *SmI* subdivisions are outlined diagrammatically in Fig. 8. All degenerative changes observed within the thalamus were ipsilateral to the unilateral neocortical ablations.

The seven planes shown in Fig. 8 are approximately those indicated in the thalamic reconstruction of Fig. 6. These data indicate that the thalamic region which degenerated after destruction of the neocortical *SmI* hindlimb and tail

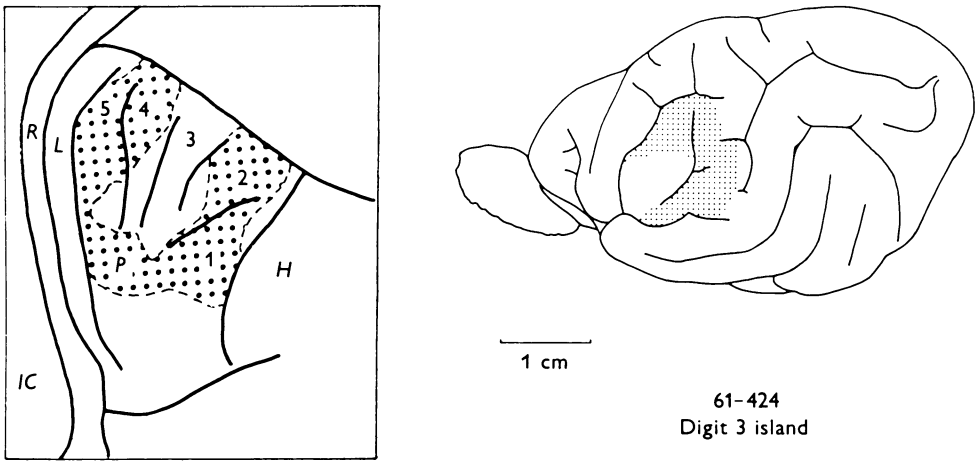

Fig. 9. Diagram (left) of horizontal section no. 611 through *Vb* complex of animal no. 61–424 showing location of thalamic degenerative changes following *SmI* neocortical ablations (dotted regions) which spared the forepaw digit 3 representation of *SmI* (right). Thalamic key diagram identifies *Vb* subdivisions and location of degenerated (dotted) regions. *H*, Head region; *L*, leg region; *IC*, internal capsule; *R*, reticular nuclear complex. Level of section within thalamus similar to that of Fig. 5 and indicated by *H–H* in Fig. 4.

subdivisions is located laterally, just medial to the thalamic reticular nuclear complex. The thalamic region showing degenerative changes after neocortical head area removal lies more medially and constitutes the arcuate subdivision of *Vb* (Fig. 8J), being bounded laterally by a thin fibrous lamina. A small subnucleus located medial to the thalamic head region did not degenerate following either total *SmI* or head area ablations, and may be the locus of termination of thalamic gustatory afferents (cf. Blomquist, Benjamin & Emmers, 1962). Similar analyses of thalamocortical connexions in other ablated brains show that representations of the five forepaw digits are arranged mediolaterally and anteroposteriorly in a manner similar to that revealed by the recording experiments.

In one animal in which unilateral ablation of neocortical representations of the distal tips of the forepaw digits had been made, the thalamic degenerative changes were located at the more anterior portions of the *Vb* digit representations. Similarly, neocortical ablation of distal palm areas resulted in degenerative changes at the more anterior portions of the *Vb* palm region.

Fig. 9 shows a diagrammatic reconstruction of a horizontal section through *Vb* in the one animal in which the *SmI* digit 3 subregion was spared while the digital and palmar neocortex surrounding it was removed. An analysis of serial horizontal sections through *Vb* in this case showed that the entire third digit subnucleus was spared of degenerative changes, whereas all of the surrounding digital subnuclei, as well as the more caudally situated palm region, exhibited considerable degeneration. Some sparing of cells occurs in each of the other forepaw digit nuclei on this section, but as will be discussed below, these spared regions were found to be associated with a sparing of portions of the homologous neocortical subregions.

All these data indicate that the pattern of organization of the *Vb* thalamic somatic sensory region, as determined by the retrograde degeneration technique was similar in all three dimensions to that disclosed by the microelectrode recording method.

Significance of thalamic lobulation. The cellular lobulations and intervening laminae within *Vb* were found to persist through several adjacent serial sections. The distinctiveness of these outlines varies in different regions, however, and is occasionally obscured by the presence of the thalamocortical fibre bundles crossing the vertically oriented lamina at right angles. The laminae and subnuclei were usually much more easily seen on sections stained for myelin sheaths than on those stained for cell bodies. All thirteen of the ablated brains showed the cellular lobules separated by thin fibrous laminae on both the normal and degenerated sides. Careful examination of the serial sections made it clear that the pattern of this lamination and lobulation was similar for all of these brains. Slight variations in the density of staining or clustering of cells, or in the adequacy of the myelin sheath stain existed among the several brains, but a common pattern of subnuclear differentiation could always be discerned in all three dimensions of the *Vb* complex. In order to determine whether these morphological features exhibited specific physiological characteristics, we compared the location of the several lobules and lamina with (*a*) the location of degenerative changes in the ablated brains and (*b*) the location of the recording loci within the electrode tracks in the brains from which evoked unit activity was recorded. These efforts led to the discovery that each morphologically distinct lobule contained the representation for a particular peripheral subdivision of the body. Not only did a particular subnucleus contain the representation of a specific body subdivision, but it selectively degenerated when its homologous neocortical representation was destroyed. Thus, the digit 3 subnucleus exhibited degeneration when the homologous neocortical region was destroyed (Fig. 4), whereas this subnucleus was spared, and surrounding subnuclei degenerated, in the neocortical digit 3 sparing case (Fig. 9). Figs. 4, 5 and 9 show drawings of sections indicating which lobule received projections from which peripheral body part.

The evidence obtained in these series of experiments shows that these subnuclei, which appear as gently curved semi-concentric sheaths of cells within the *Vb* complex, do not represent the projections of spinal dermatomes or spinal segments as has been suggested by Chang & Ruch (1947) for the spider monkey, Mountcastle & Henneman (1952) for the rhesus monkey and Mountcastle & Henneman (1949) and Rose & Mountcastle (1959) for the cat. Rather, each lobule contains the

thalamic representation for mechanoreceptors from a particular peripheral body part. The subnuclei of the ventro-basal group in the raccoon thus seem to be differentiated from one another on the basis of source of peripheral afferents.

A previous study has shown that the fractionation of raccoon somatic sensory cerebral cortex by fissures and sulci has occurred on a similar basis (Welker & Seidenstein, 1959; and Fig. 10). All these data indicate that *SmI* neocortex and

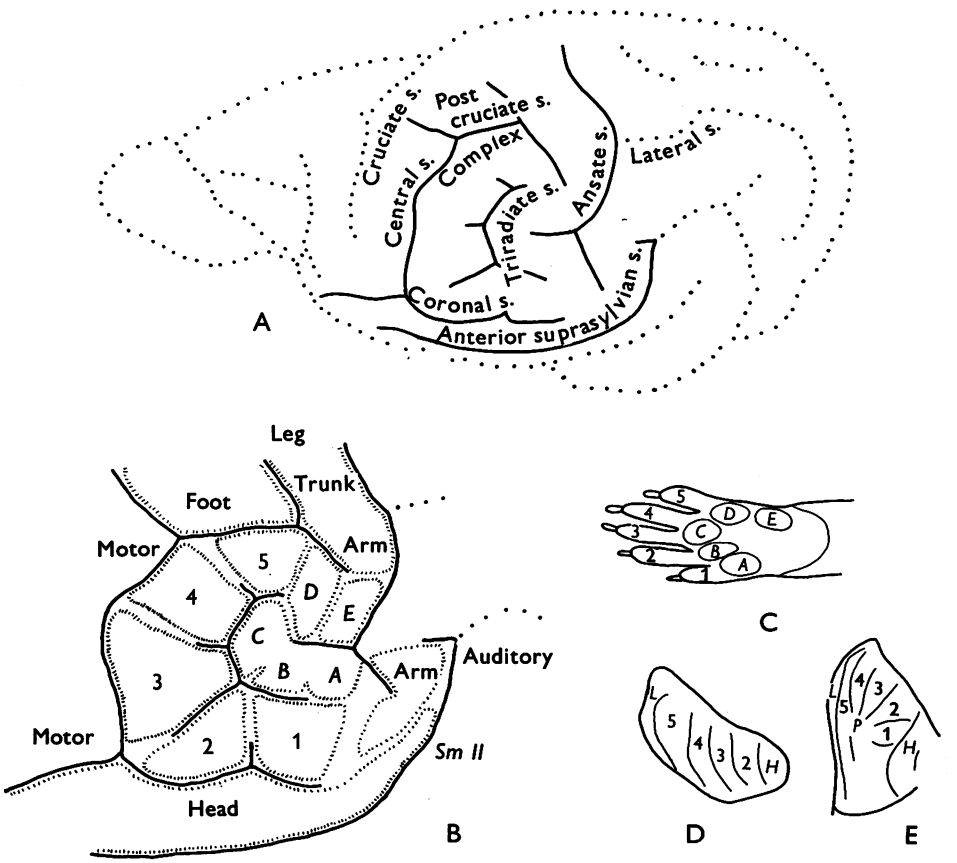

Fig. 10. A, Left dorso-lateral view of raccoon brain in outline. Solid lines indicate sulci which lie within and around *SmI* neocortex. B, Representation of major body subdivisions within and around elliptical forepaw region of *SmI* neocortex. Each subdivision surrounded by bearded line. Solid lines indicate sulci and correspond to those in A. C, drawing of left ventral forepaw and its subdivisions. Note similarity of somatotopic organization of peripheral forepaw subdivisions and their cortical representations. D and E, schematic diagrams of coronal and horizontal sections through *Vb* similar to key diagrams in Figs. 4 and 5. Symbols similar to those in these latter figures.

Vb thalamus are divided into subregions at homologous zones within the somatotopic pattern. Although most neocortical sulci within and around *SmI* are paralleled by fibrous lamina at homologous loci within and around *Vb*, this association is not always found. Thus, a neocortical sulcus may exist without the coexistence of a corresponding thalamic lamina. The reverse also occurs. Thus fibrous lamina *may*

occur within *Vb* in the absence of a corresponding neocortical sulcus at a homologous location. Moreover, as can be seen in Fig. 10, a large lamina in *Vb* may be associated with only a small sulcal spur or dimple at *SmI* (e.g. compare the region between the digit 3 and 4 representations at both thalamus and neocortex). The absence of fissures within certain regions of *SmI* (e.g. within the head or trunk representations) are paralleled by a similar lack of clear fibrous laminae within the homologous *Vb* regions.

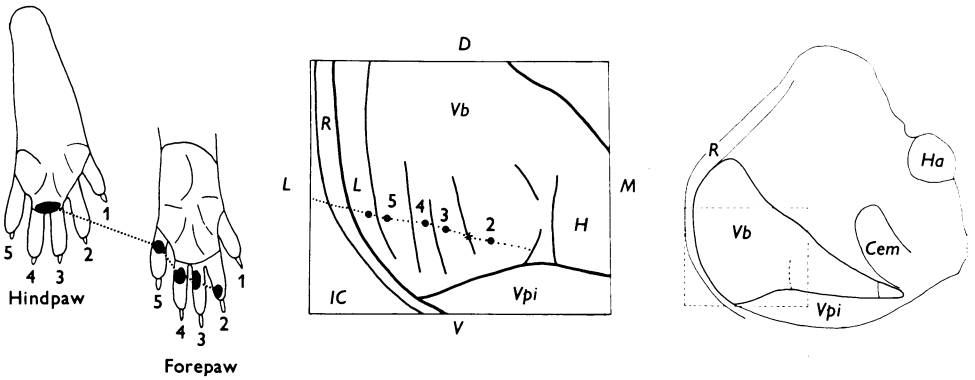

Fig. 11. Diagrams of coronal section (right) no. 119 of left thalamus of raccoon no. 63–91 showing horizontal course of tungsten microelectrode track no. 4 through *Vb* subnuclei (centre) which contain representations of indicated body subdivisions. *L*, *5*, *4*, *3*, *2* and *H* refer to hindlimb, forpaw digit, 5, 4, 3, 2 and head subdivisions respectively. Dotted line in centre diagram indicates location of electrode track. Large dots on this line in the diagram indicate recording locations. Asterisk (*) indicates location of microlesion between representations of forepaw digits 2 and 3. Microlesion produced by passing 1·5 V d.c. through tungsten electrode tip. Black patches on figurines at left indicate peripheral receptive fields mechanical stimulation of which evoked unit clusters at the successively latero-medial locations in *Vb*. Note *disjunctive shift* of receptive fields from one distinct body part to another as electrode crosses successive fibre laminae. *Cem*, centromedian nucleus; *Ha*, habenular nuclear complex; *IC*, internal capsule; *R*, thalamic reticular complex; *Vb*, ventro-basal nuclear complex; *Vpi*, ventral posterior-inferior nucleus; *D*, *V*, *L*, *M*, dorsal, ventral, lateral, medial.

Of special interest to us was the fact that at the caudo-lateral aspect of *Vb* a pronounced but thin subnucleus was found which appears to contain the representation for the tail. This thin crescent-shaped band of cells is separated from the hindlimb lobule by a fibrous lamina, and appears on only a few sections in each brain examined. Its point of attachment to the rest of the ventro-basal group is rather high laterally at a locus where, in one experiment (no. 62–522), the microelectrode recorded from cells activated by stimulation of the base of the tail and perianal region. Stimulation of the tip of the tail activated cells more ventrally and caudally within this tail lobule.

These morphological data provide an explanation for the results presented above regarding the continuous and disjunctive shifts of representation which were obtained during the passage of the electrode through the thalamic somatic sensory region. Examination of the course of these electrode tracks through the thalamus showed that a *disjunctive shift* occurred at locations where the recording electrode

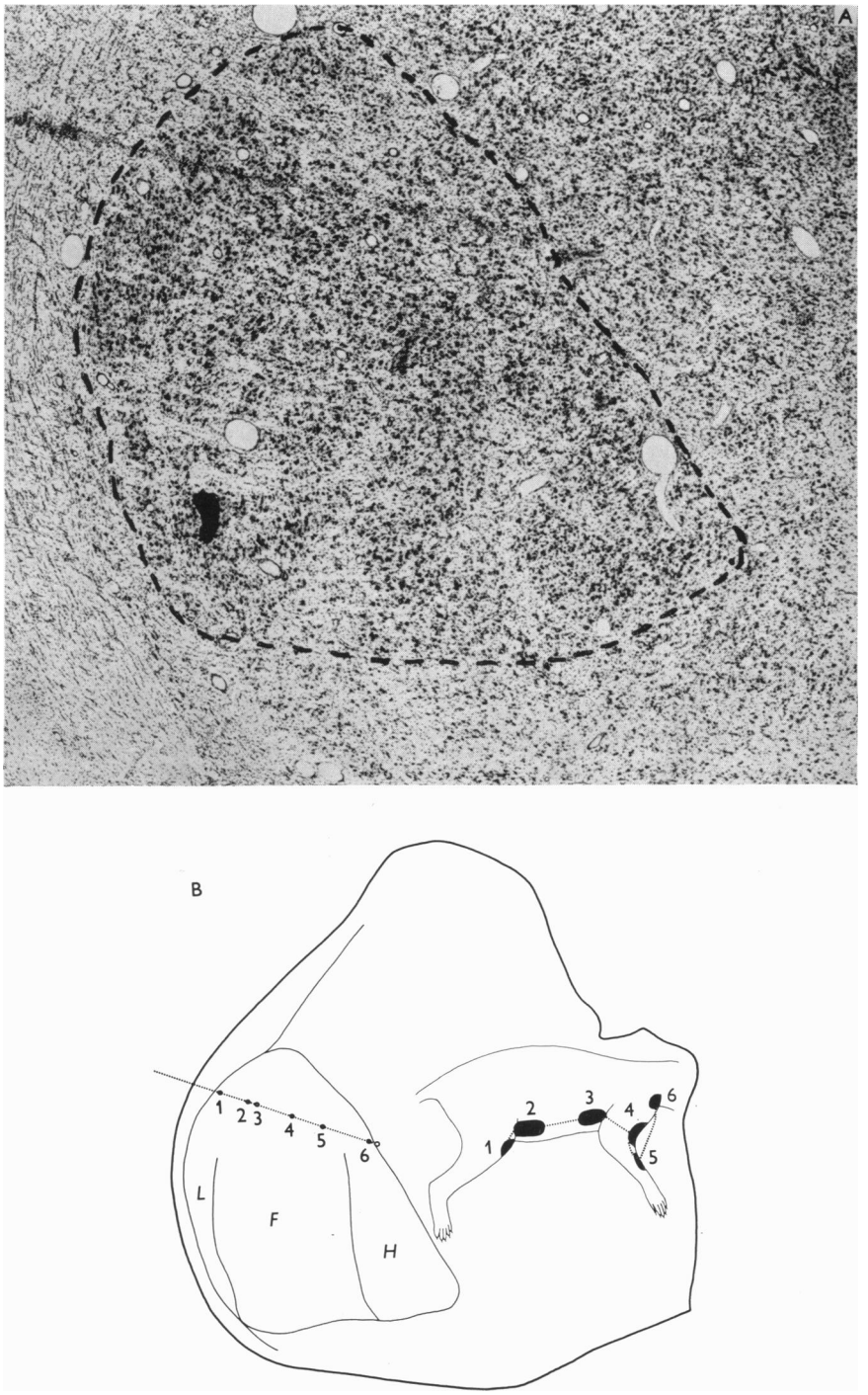
A
B
1
2
3
4
5
6
L
F
H
1
2
3
4
5
6

tip crossed a fibrous lamina during its passage from one subnucleus to another. When such a shift occurred there was usually a relatively quiet zone of low amplitude activity between the two regions on either side from which large amplitude unit spike clusters could be evoked and recorded. A *continuous shift* occurred, however, when the electrode tip passed through a non-lobulated, non-laminar region. As might be expected, since the fibre fascicles and subnuclei are oriented in a dorsoventral plane, horizontal electrode punctures through the lower regions of *Vb*

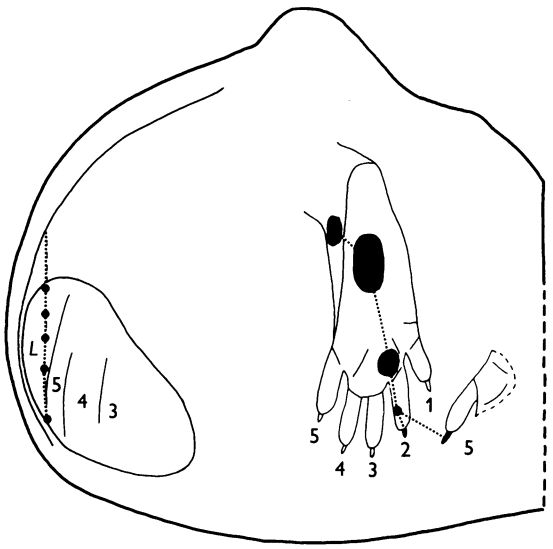

Fig. 13. Diagrammatic reconstruction of section through left thalamus of raccoon no. 62–557. Electrode puncture no. 8 indicated by dotted line. Large dots on this line indicate recording locations activated by mechanical stimulation of the receptive fields indicated on figurines at the right. Note continuous shift of receptive fields along foot as electrode descends within the hindlimb subnucleus. The deepest recording location lay within a fibre lamina and small unit spikes were recorded here from stimulation of claws of both hind foot digit 2 and forepaw digit 5.

resulted in a greater proportion of disjunctive than continuous shifts. Fig. 11 shows such a case in which the electrode passed through five distinct *Vb* subnuclei and in which the receptive fields activating *Vb* units shifted disjunctively from one body part to another. The fibre fascicles do not extend into the more dorsal portions of *Vb*, and horizontal electrode punctures into this region resulted primarily in continuous shifts (Fig. 12).

Fig. 12. A, Section no. 138 through thalamus of raccoon no. 63–91. Line of gliosis indicates electrode track no. 1. Boundary of *Vb* at this level indicated by dashed line. Thionin stain. ×24. B, Figurine at right interpreted similar to that in Fig. 11. Note recording electrode track passes through non-lobulated dorsal region of *Vb*. As the recording electrode tip passed latero-medially through the successively numbered thalamic loci, the activating receptive fields shifted *continuously* up the hindlimb, on to and forward along the trunk, and down on to the forelimb. The shift between locations 5 and 6 was discontinuous as the electrode passed just above the arcuate fibre lamina. Open circle at end of track indicates location of microlesion placed at boundary of *Vb*. *L*, *F*, *H*, Leg, forepaw, and head subdivisions of *Vb*.

An electrode entering the thalamus from above more commonly remained within a particular subnucleus throughout its dorso-ventral course, and in such cases receptive fields shifted in continuous fashion (Fig. 13). In experiments where iron deposits or microlesions were placed between two adjacent regions exhibiting a disjunctive shift, these marks were centered within a fibre lamina between two subnuleic (Fig. 11).

As is usually the case in chronic ablation experiments, the extent of the neocortical removals was not always exactly as intended. Since each of the neocortical sulci, spurs, and dimples within and around the raccoon's *SmI* has been shown to delimit reliably one *SmI* subdivision from another (Fig. 10), it was usually possible during reconstruction of the neocortical lesions to determine which portions of the somatotopic pattern had been spared. The removal of more cortex than was intended could also be identified with respect to its location within the somatotopic pattern. Such errors in ablation were invaluable since they provided a series of tests of hypotheses regarding the thalamic locations of minor features of the somatotopic pattern. It was found, for example, that when the distal, radial portion of the third forepaw region was spared in *SmI*, cells in the homologous portion of the third digit lobule within the thalamic *Vb* complex were also selectively spared. A similar thalamocortical correspondence in relative position and location of small portions of the somatotopic pattern were found for ulnar digit 5, proximal digit 5, distal ventral digit 4, proximal digit 4, proximal ulnar digit 2, radial digit 2 and palm pads *A* and *E* (cf. Figs. 8 and 9). In each of two cases (D and H in Fig 8) the location of a small unintended neocortical lesion was predicted, and subsequently verified, when thalamic degenerative changes were discovered in a small region separated from that which was related to the primary lesion.

No clear degenerative changes were found within the thalamus of raccoon no. 62–511 following ablations of portions of the shoulder, hip, trunk, tongue, or tail subdivisions. These neocortical ablations were relatively small and the absence of pronounced degenerative changes suggests the presence of some degree of sustaining projections within these regions (cf. Rose & Woolsey, 1958).

Degeneration outside the ventro-basal complex. The nucleus ventralis posterior inferior (*Vpi*) did not show clear degenerative changes in any of the animals in which portions of *Vb* tissue just above it exhibited marked degeneration, although it showed some alteration in the hemidecorticate animal. The thalamic reticular nuclear complex did not show obvious degenerative changes in any of the cases with selective partial ablations of *SmI*. However, this nuclear complex did show degenerative changes in the total *SmI* and total neocortical ablations. These findings corroborate those of Rose (1950) and Chow (1952) in showing that degenerative changes in the reticular nuclear complex are minimal with small neocortical ablations and more pronounced with larger neocortical ablations. In both animals in which the total neocortical *SmI* was ablated, adjacent neocortex behind the ansate sulcus was also invaded. In both these cases, degenerative changes were visible in the lateral nuclear complex just above the external portion of *Vb*. In animal no. 61–639 fibres passing to the medial wall of the hemisphere were interrupted, and in this case degenerative changes were apparent in the anterior ventral nucleus on that side. As long as the neocortical ablations were kept within neo-

cortical *SmI*, degenerative changes were confined to the ventro-basal nuclear complex.

Somatotopic pattern in three dimensions. A schematic three dimensional reconstruction of *Vb* is presented in Fig. 14. This drawing represents a summary of the

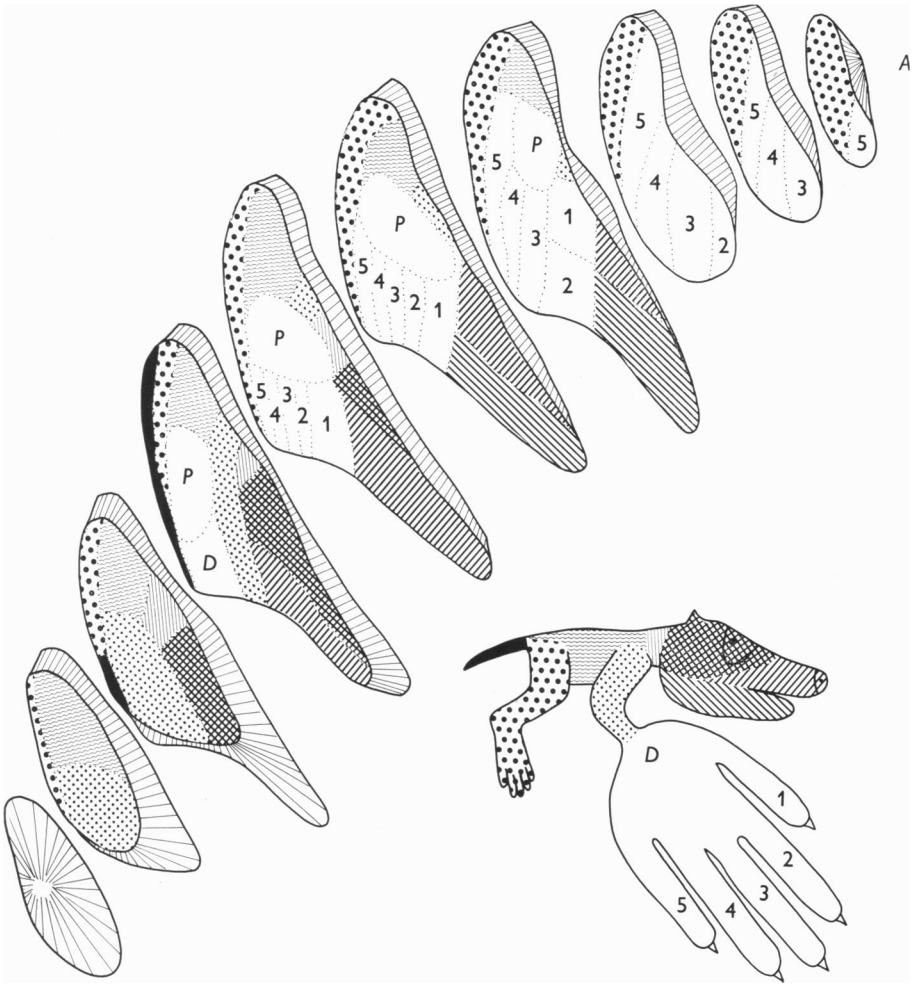

Fig. 14. Schematic three dimensional drawing of *Vb* nuclear complex of raccoon no. 57–88 summarizing location of thalamic representations of several body subdivisions as determined by electrophysiological mapping and retrograde degeneration experiments. Figurine at right gives key to body subdivisions and indicates their relative degree of enlargement within *Vb*. *D*, Dorsum of forepaw; *P*, palm of forepaw, not shown in figurine. Sections through *Vb* oriented as are those in Fig. 6. *A*, Anterior.

electrophysiological and neuroanatomical data, and is intended to facilitate visualization of the somatotopic organization within *Vb*. This figure illustrates more clearly than the previous figures the distorted character of the procyonculus at the thalamic nuclear level of the medial lemniscal somatic sensory system.

Quantitative studies. Since both the *Vb* thalamic, and *SmI* neocortical, regions are demarcated by anatomical landmarks which separate several specific somatic sensory representations, we were able to obtain estimates of the absolute and relative volumes of these subdivisions in normal sections. In order to illustrate one use of quantitative neuroanatomical methods, we compared the relative nuclear volumes (measured by methods described by Dornfeld, Slater & Scheffé, 1942) of three major somatic sensory subdivisions (head, forepaw, all else) within both *Vb* and *SmI*.

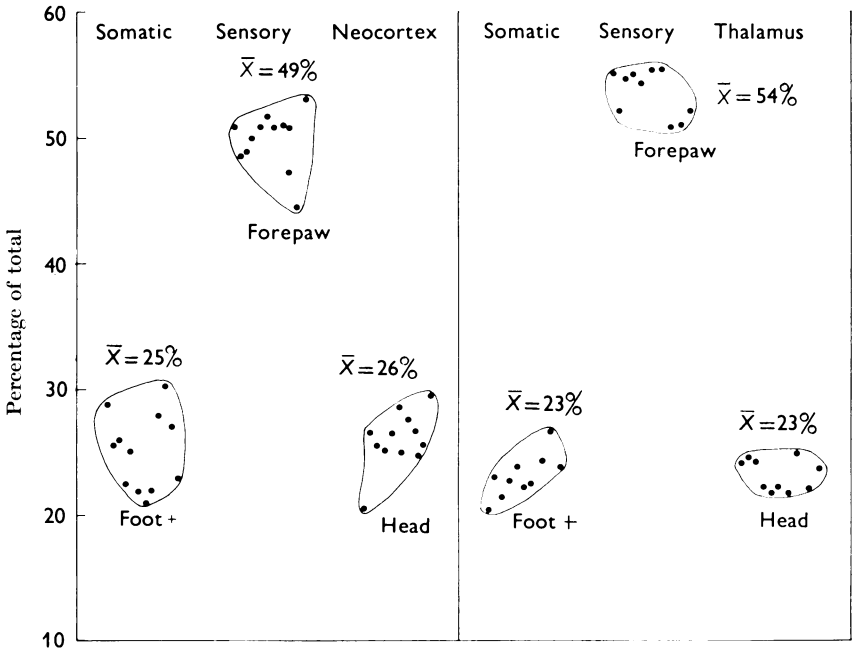

Fig. 15. Graph comparing percentages of three major subdivisions of somatic sensory regions at thalamic *Vb* (N = 10) and neocortical *SmI* (N = 12) levels of MLS. Measurements computed from planimetry of drawings of these three regions (head, forepaw, and the rest of the body taken together with that of the foot) in normal right hemispheres. $\bar{X}$, Mean.

Fig. 15 illustrates the results of this comparison and shows that the proportions of the total somatic sensory region devoted to a particular major subdivision is similar at thalamus and neocortex. The average proportion of *Vb* occupied by the forepaw representation is somewhat larger than that reported above for one of the recording experiments (no. 61–148). The degree to which variable brain size, differential shrinkage during histological processing, errors in microscopic identification of subdivisions of *Vb* and *SmI* and, true intrageneric variations, contribute to the observed variations in relative volumes within these regions cannot be answered from our available data.

DISCUSSION

Definition of thalamic level of MLS. Our data for the raccoon confirm the conclusions of Rose & Mountcastle (1959) that the ventro-basal nuclear complex of the thalamus: (*a*) coincides with the thalamic terminations of the medial lemniscus, (*b*) is activated by light mechanical stimulation of somatic sensory mechanoreceptors, and (*c*) sends projections to *SmI* neocortex. However, it should be remembered that the dorsal column nuclei are not the only sources of somatic sensory input to *Vb* since several studies have shown that axon terminals from the spinothalamic pathways make contact with *Vb* (Bowsher, 1958, 1961; Chang & Ruch, 1947; Mehler, Feferman & Nauta, 1960; Perl & Whitlock, 1961; Whitlock & Perl, 1961), although the mode of termination here may be different for axons from the two pathways (Bowsher, 1961; Mehler *et al.* 1960).

Another complication in the circuitry of the MLS within diencephalic regions is suggested by the fact that some *Vb* cells are left intact following total removal of *SmI* or even after hemidecortication. That the projection of *Vb* cells to homologous neocortical cells is not of a simple, direct nature, and probably involves some sort of sustaining or collaterel penetration of *SmI*, is suggested by the predominance of shrunken cells with no apparent cell loss within *Vb* in those cases in this study where neocortical lesions were small (cf. Clark & Powell, 1953).

Our data indicate that the laminar and lobular characteristics of *Vb* are primarily related to the mode of termination of its medial lemniscal afferents from specific peripheral body subdivisions. Studies of anterograde degeneration (Marchi method) indicate that there is a considerable degree of mixing of fibres activated by the several discrete peripheral body regions within the medial lemniscus (Clark, 1936; Matzke, 1951). When these fibres reach the *Vb* nuclear complex, however, a resorting apparently occurs as the axons approach the thalamic cells upon which they terminate. We believe that the vertically oriented laminae within *Vb* are the resorting zones, or planes of segregation, for the afferent fibres to this somatic sensory thalamic region.

Thalamic lobulation and lamination in various degrees have been observed in the *Vb* region of several mammals, including humans (Cooper, 1950). They can be seen in several atlases of the brains of cat (Jasper & Ajmone-Marsan, 1954; Jiminez-Castellanos, 1949; Snider & Niemer, 1961), dog (Singer, 1962), and rhesus monkey (Olszewski, 1952; Snider & Lee, 1961). We have seen subnuclei separated by fibrous laminae in what appear to be homologous somatic sensory thalamic regions of the domestic dog and cat, mountain lion, African lion, coatimundi, kinkajou, lesser panda, mongoose, mink, harbour seal, northern fur seal, capybara, porcupine, grey squirrel, domestic pig and sheep, zebra, galago, slow loris, lemur, squirrel monkey, rhesus monkey, and gibbon. Whether these laminae have similar segregating characteristics in these animals as they do in the raccoon remains, of course, to be determined. Both Poliak (1932) and Clark (1932) suggested that such lamination and lobulation might have some functional significance.

Somatotopic organization within Vb. The pattern of organization of projections from peripheral body receptors is generally similar in the raccoon to that found in the thalamus of rats (Emmers & Leeb, 1963), rabbits (Rose & Mountcastle

1952), domestic cats (Mountcastle & Henneman, 1949; Rose & Mountcastle, 1952), and rhesus monkeys (Mountcastle & Henneman, 1952; Rose and Mountcastle, 1959). Although the topographic organization of this pattern is considerably distorted, it resembles that at the body periphery in each of these animal types. Despite these general similarities, however, the somatotopic pattern in the raccoon's *Vb* complex exhibits certain specific differences in shape and orientation from that found in these other animals. For example, the tail region within *Vb* is located caudo-laterally in the raccoon, and antero-laterally in the cat (Mountcastle & Henneman, 1949).

Of greater probable functional significance than the general three-dimensional orientation of the body representation within the thalamus is the maintenance of an organized somatotopic pattern of representation at thalamic, as well as at all other, nuclear levels of the MLS. The fact that 'surround inhibition', which is believed to be a manifestation of a mechanism promoting perceptual acuity (Békésy, 1958, 1959; Granit, 1955; McIntyre, 1963; Mountcastle & Powell, 1959), occurs primarily from the neighbouring peripheral receptive fields may be related to the fact that the receptive fields of adjacent body parts are represented adjacent to one another within cuneate-gracile, ventro-basal, and *SmI* neocortical nuclear complexes. We believe that this *organized contiguity of representations* may be associated with the increased probability of establishment of those anatomical interconnexions which presumably underly the phenomena of afferent inhibition.

The MLS *and behaviour.* Our studies of the somatic sensory system in raccoons grew out of a realization that these animals exhibit a pronounced behavioural specialization with respect to their use of the forepaws in palpation, manipulation, and exploration of objects and surfaces (cf. Lyall-Watson, 1963). The forepaw representations in this animal have been found to be relatively large, as well as highly differentiated, at neocortical *SmI* (Welker & Seidenstein, 1959), thalamic *Vb* (see above), and cuneate-gracile (Johnson, Welker & Pubols, in preparation) nuclear levels of the MLS. The raccoon also exhibits a relatively large receptor density in its cutaneous forepaw tissues (Zollman & Winkelmann, 1962), as well as a relatively large population of dorsal root ganglia and axons in its cervical dorsal roots which derive from receptive fields in the forepaw (Pubols, Welker & Johnson, 1965). The relatively large forepaw regions at each of these neural levels consist primarily of the representations of the ventral glabrous surfaces of the forepaw. It appears, therefore, that the forepaw behavioural specialization of the raccoon has at least one type of CNS counterpart in the specialization of forepaw representation within the MLS. Possible roles of this differentially enlarged system in somatic sensory perception have been discussed elsewhere (Welker *et al.* 1964).

Methodological problems. The data presented above have shown that there is very little overlap between several thalamic representations from anatomically separate peripheral body parts. A comparison of the *macro*electrode slow-wave evoked potential, and the *micro*electrode evoked unit-cluster mapping experiments, showed that these two methods produce different results as regards: (*a*) the degree of differentiation of the pattern of representation, (*b*) the relative size of the representations of peripheral receptive fields, and (*c*) the degree of overlap of representation of these fields at adjacent thalamic loci. Since the microelectrode unit cluster

method increased the specificity of representation in all these respects, we have assumed that the spread of pick-up, which occurs within a volume conductor, is sufficiently pronounced, when macroelectrodes are used, to increase the apparent degree of overlap (Woodbury, 1962). Consequently we believe that the evoked slow wave potential cannot be used to identify fine details in a responding population of neurons since it consists of the summation of potentials of numerous sources and sinks from numerous neural structures at variable distances from the recording electrode (Lorente de Nó, 1947). Possibly, the use of a single-unit, instead of a unit-cluster, criterion would result in even more precision in localization patterns than we have found in this study. The amount of overlap of adjacent projections from head and forepaw reported for the thalamus of rabbits (Rose & Mountcastle, 1952), cats (Mountcastle & Henneman, 1949), and rhesus monkeys (Mountcastle & Henneman, 1952) may have been influenced by this factor since macroelectrodes and slow-wave response criteria were used in those recording studies. Mountcastle & Henneman (1949) were aware of this problem, and they observed that the apparent degree of localization was greater if recording electrodes with relatively small exposed surface area were used. Until these regions are examined with microelectrodes in these various animals, uncertainty will persist regarding whether the different degrees of overlap obtained in such experiments represent valid generic differences or are in part due to spread-of-pickup artefacts.

Another related methodological issue concerns the method of body stimulation used in studying projection patterns of somatic sensory receptors. Since many of the mechanoreceptors which project into the MLS are exquisitely sensitive to light mechanical stimulation (cf. Pubols *et al.* 1965), great care is required to minimize activation of distant receptors by mechanical spread of the stimulus through intervening tissue. Thus, the stronger the peripheral mechanical stimulus, the larger will be the apparent size of the receptive field. This stimulation artefact, together with the artefact inherent in the use of the evoked slow-wave potential response criterion, would tend to increase the apparent overlap, thereby resulting in relatively poorer differentiation or specificity of the somatotopic pattern of peripheral projections. These observations suggest that, in studies seeking to define patterns of connections between two cellular mosaics (e.g. receptors and thalamic *Vb*) with maximum resolution of detail, it is essential to employ not only systematic mapping techniques, but unit response criteria, as well as great care in preventing mechanical spread of the peripheral stimulus.

SUMMARY

The thalamic ventro-basal (*Vb*) nuclear level of the raccoon's medial lemniscal system (MLS) was studied by electrophysiological recording and retrograde degeneration methods. These methods were used to define certain relationships of this nuclear complex both to peripheral somatic sensory receptors and to the somatic sensory neocortex in a total of 31 raccoons.

The aggregation of cells within the raccoon's *Vb* complex into subnuclei separated by fibre laminae was found to be organized on a somatotopic basis, such that distinct adjacent subnuclei were activated by mechanical stimulation of distinct

body regions which are also adjacent to one another. These physiological-morphological correlations are associated with the high degree of differentiation of the raccoon's thalamic forepaw representation.

The somatotopic organization of the pattern of representation of peripheral receptors was found to be similar to that described for other mammals, but, as at the raccoon's *SmI* neocortex, its *Vb* thalamic representation of glabrous forepaw surfaces is unusually large, accounting for almost 50% of the *Vb* volume. The somatotopic pattern of organization of thalamocortical connexions as defined by the retrograde degeneration method confirmed in every respect the pattern defined by the electrophysiological recording method.

This research was supported by Grants from the National Institutes of Health (M-2786 and B-3249), and from the Research Committee of the University of Wisconsin out of funds provided by the Wisconsin Alumni Research Foundation. The authors would like to express their appreciation to C. N. Woolsey for performing one of the cortical ablations; to G. B. Campos, B. H. Pubols, Jr., C. Thompson, C. Welt, J. Brugge, D. Musolf, and A. Miller for their assistance in some of the physiological recording or ablation experiments; to Helen Brandemuehl and Isabel Lucey for their fine histological preparation of the brain materials; and to T. P. Stewart for his assistance in preparation of the photomicrograph and other graphic materials.

REFERENCES

AKERT, K. & WELKER, W. I. (1961). Problems and Methods of Anatomical localization. In *Electrical Stimulation of the Brain*, chap. 17, pp. 251–260. Ed. D. E. Sheer. Austin, Texas: University of Texas Press.

BEKÉSY, G. V. (1958). Funneling in the nervous system and its role in loudness and sensation intensity on the skin. *J. acoust. Soc. Am.* **30**, 399–412.

BEKÉSY, G. V. (1959). Similarities between hearing and skin sensations. *Psychol. Rev.* **66**, 1–22.

BISHOP, P. O., BURKE, W. & DAVIS, R. (1962). The interpretation of the extracellular response of single lateral geniculate cells. *J. Physiol., Lond.* **163**, 451–472.

BISHOP, P. O., KOZAK, W., LEVICK, W. R. & VAKKUR, G. J. (1962) The determination of the projection of the visual field on to the lateral geniculate nucleus in the cat. *J. Physiol., Lond.* **163**, 503–539.

BLOMQUIST, A. J., BENJAMIN, R. M. & EMMERS, R. (1962) Thalamic localization of afferents from the tongue in squirrel monkey (*Saimiri sciureus*). *J. comp. Neurol.* **118**, 77–87.

BOWSHER, D. (1958). Projection of the gracile and cuneate nuclei in *Macaca mulatta;* an experimental degeneration study. *J. comp. Neurol.* **110**, 135–155.

BOWSHER, D. (1961). The termination of secondary somatosensory neurons within the thalamus of *Macaca mulatta*: an experimental degeneration study. *J. comp. Neurol.* **117**, 213–227.

CHANG, H.-T & RUCH, T. C. (1947). Topographical distribution of spinothalamic fibres in the thalamus of the spider monkey. *J. Anat.*, **81**, 150–164.

CHOW, K. L. (1952). Regional degeneration of the thalamic reticular nucleus following cortical ablations in monkeys. *J. comp. Neurol.* **97**, 37–59.

CLARK, W. E. LE GROS. (1932). The structure and connections of the thalamus. *Brain*, **55**, 406–470.

CLARK, W. E. LE GROS. (1936). The termination of ascending tracts in the thalamus of the macaque monkey. *J. Anat.*, **71**, 7–40.

CLARK, W. E. LE GROS & POWELL, T. P. S. (1953). On the thalamo-cortical connexions of the general sensory cortex of Macaca. *Proc. R. Soc.* B, **141**, 467–487.

COOPER, E. R. A. (1950). The development of the thalamus. *Acta anat.* **9**, 201–226.

DORNFELD, E. J., SLATER, D.W. & SCHEFFÉ, H. (1942). A method for accurate determination of volume and cell numbers in small organs. *Anat. Rec.* **82**, 255–259.

EMMERS, R. & LEEB, I. J. (1963). Patterns of somesthetic representation in SI and SII in the rat thalamus. *Fedn Proc. Fedn Am. Socs exp. Biol.* **22**, 394 (abstract).

FATT, P. (1957). Electrical potentials occurring around a neurone during its antidromic activation. *J. Neurophysiol.* **20**, 27–60.

FREYGANG, W. H., JR. (1958). An analysis of extracellular potentials from single neurons in the lateral geniculate nucleus of the cat. *J. gen. Physiol.* **41**, 543–564.

GRANIT, R. (1955). *Receptors and Sensory Perception.* New Haven, Connecticut: Yale University Press.

GREEN, J. D. (1958). A simple microelectrode for recording from the central nervous system. *Nature, Lond.*, **182**, 962.

HUBEL, D. H. (1957). Tungsten microelectrode for recording from single units. *Science*, **125**, 549–550.

JASPER, H. H. & AJMONE-MARSAN, C. (1954). *A Stereotaxic Atlas of the Diencephalon of the Cat.* Ottawa: National Research Council of Canada.

JIMENEZ-CASTELLANOS, J. (1949). Thalamus of the cat in Horsley-Clarke coordinates. *J. comp. Neurol.* **91**, 307–330.

JOHNSON, J. I., JR., WELKER, W. I. & PUBOLS, B. H., JR. (1966). Somatotopic organization in raccoon dorsal column nuclei (manuscript in preparation).

LORENTE DE NÓ, R. (1947). A study of Nerve Physiology. *Stud. Rockefeller Inst. med. Res.* **131**, and **132**.

LYALL-WATSON, M. (1963). A critical re-examination of food "washing" behaviour in the raccoon (*Procyon lotor* Linn.). *Proc. zool. Soc. Lond.*, **141**, 371–395.

MATZKE, H. A. (1951). The course of the fibers arising from the nucleus gracilis and cuneatus of the cat. *J. comp. Neurol.* **94**, 439–452.

MCINTYRE, A. K. (1963). Coding of sensory input. *Aust. J. Sci.* **25**, 397–403.

MEHLER, W. R., FEFERMAN, M. E. & NAUTA, W. J. H. (1960). Ascending axon degeneration following anterolateral cordotomy. An experimental study in the monkey. *Brain*, **83**, 718–752.

MOUNTCASTLE, V. B. & HENNEMAN, E. (1949). Pattern of tactile representation in thalamus of cat. *J. Neurophysiol.* **12**, 85–100.

MOUNTCASTLE, V. B. & HENNEMAN, E. (1952). The representation of tactile sensibility in the thalamus of the monkey. *J. comp. Neurol.* **97**, 409–439.

MOUNTCASTLE, V. B. & POWELL, T. P. S. (1959). Neural mechanisms subserving cutaneous sensibility, with special reference to the role of afferent inhibition in sensory perception and discrimination. *Johns Hopkins Hosp. Bull.* **105**, 201–232.

OLSZEWSKI, J. (1952). *The Thalamus of the Macaca mulatta. An Atlas for Use with the Stereotaxic Instrument.* Basel: S. Karger.

PERL, E. R. & WHITLOCK, D. G. (1961). Somatic stimuli exciting spinothalamic projections to thalamic neurons in cat and monkey. *Expl Neurol.* **3**, 256–296.

POLIAK, S. (1932). The main afferent fiber systems of the cerebral cortex in primates. *Univ. Calif. Publ. Anat.* **2**, 1–370.

PUBOLS, B. H., JR., WELKER, W. I. & JOHNSON, J. I., JR. (1965). Somatic sensory representation of forelimb in dorsal root fibers of raccoon, coatimundi, and cat. *J. Neurophysiol.* **28** (in the Press).

ROBINSON, B. W. (1962). Localization of intracerebral electrodes. *Expl Neurol.* **6**, 201–223.

ROSE, J. E. (1950). The cortical connections of the reticular complex of the thalamus. *Proc. Ass. Res. nerv. ment. Dis.* **30**, 454–479.

ROSE, J. E. & MOUNTCASTLE, V. B. (1952). The thalamic tactile region in rabbit and cat. *J. comp. Neurol.* **97**, 441–489.

ROSE, J. E. & MOUNTCASTLE, V. B. (1954). Activity of single neurons in the tactile thalamic region of the cat in response to a transient peripheral stimulus. *Johns Hopkins Hosp. Bull.* **94**, 238–282.

ROSE, J. E. & MOUNTCASTLE, V. B. (1959). Touch and kinesthesis. In *Handbook of Physiology. Section I. Neurophysiology*, vol. 1, chap 17. Ed. J. Field, H. W. Magoun and V. E. Hall. Washington, D.C.: American Physiological Society.

ROSE, J. E. & WOOLSEY, C. N. (1958). Cortical connections and functional organization of the thalamic auditory system of the cat. In *Biological and Biochemical Bases of Behavior*, pp. 127–150. Ed. H. F. Harlow and C. N. Woolsey. Madison, Wisconsin: University of Wisconsin Press.

SINGER, M. (1962). *The Brain of the Dog in Section.* Philadelphia: Saunders.

SNIDER, R. S. & LEE, J. C. (1961). *A Stereotaxic Atlas of the Monkey Brain.* Chicago: University of Chicago Press.

SNIDER, R. S. & NIEMER, W. T. (1961). *A Stereotaxic Atlas of the Cat Brain.* Chicago: University of Chicago Press.

SVAETICHIN, G. (1958). Component analysis of action potentials from single neurons. *Expl Cell Res.* (Suppl.) **5**, 234–261.

SWANK, R. L. & DAVENPORT, H. A. (1935). Chlorate-osmic-formalin method for staining degenerating myelin. *Stain Tech.* **10**, 87–90.

TASAKI, I., POLLEY, E. H. & ORREGO, F. (1954). Action potentials from individual elements in cat geniculate and striate cortex. *J. Neurophysiol.* **17**, 454–474.

WELKER, W. I., JOHNSON, J. I., JR. & PUBOLS, B. H., JR. (1964). Some morphological and physiological characteristics of the somatic sensory system in raccoons. *Am. Zool.* **4**, 75–94.

WELKER, W. I. & SEIDENSTEIN, S. (1959). Somatic sensory representation in the cerebral cortex of the raccoon (*Procyon lotor*). *J. comp. Neurol.* **111**, 469–501.

WHITLOCK, D. G. & PERL, E. R. (1961). Thalamic projections of spinothalamic pathways in monkey. *Expl Neurol.* **3**, 240–255.

WHITNEY, L. F. & UNDERWOOD, A. B. (1952). *The Raccoon.* Orange, Connecticut: Practical Sciences Publishing Co.

WOODBURY, J. W. (1962). Potentials in a volume conductor. In *Neurophysiology*, pp. 83–91, Ed. T. C. Ruch, H. D. Patton, J. W. Woodbury and A. L. Towe. Philadelphia: Saunders.

WOOLSEY, C. N. (1958). Organization of somatic sensory and motor areas of the cerebral cortex. In *Biological and Biochemical Bases of Behavior*, pp. 63–81. Ed. H. F. Harlow and C. N. Woolsey. Madison, Wisconsin: University of Wisconsin Press.

ZOLLMAN, P. E. & WINKELMANN, R. K. (1962). The sensory innervation of the common North American Raccoon (*Procyon lotor*). *J. comp. Neurol.* **119**, 149–157.